EAN 2017
55th conference on experimental stress analysis

Methodology for probabilistic model creation of lidar measurement

Dekan Martin[1,a], Chovanec Luboš[1,b], Szabová Martina[1,c] and Babinec Andrej[1,d]

[1]Faculty of Electrical Engineering and Information Technology STU in Bratislava, Ilkovičova 3, Bratislava, Slovakia

[a]martin.dekan@stuba.sk, [b]lubos.chovanec@stuba.sk, [c]martina.szabova@stuba.sk, [d]andrej.babinec@stuba.sk

Keywords: Probabilistic model, laser rangefinder, mixed pixel.

Abstract. The core of this article comprises several approaches to probabilistic modeling of Hokuyo type LRF. Motivation for creating these models was the failure to faithfully represent LRF features in existing models. Moreover, the use of mixed pixel error as a mean of laser rangefinder identification is described.

Introduction

Nowadays, mobile robots preform their operations in dynamically changing environment. That is why they need to sense this environment with powerful and reliable sensors, which can provide sufficient amount of data. Historically there are many sensors used for environment sensing. However, for reliable and effective navigation of the robot the laser rangefinders (LRF) are mostly used. Due to continual decline in price they are already used in hobby robotics or in service robots for domestic tasks [1]. When working with a sensor it is necessary to know the principle of sensor's measurement and its properties[9,11]. There are several measurement principles used in LRFs [2,3] precisely triangulation, time of flight (TOF), frequency modulation continuous wave (FMCW) and phase shift measurement (PSM). These measurement principles are well known and the details about them can be found in [1] or in [2]. Properties of LRF can be defined as product details, but they can be extended by properties, which are not defined by producer. Such not well defined properties may be represented by measurements to other materials than those mentioned in catalogue or by measurements when LRF fails [3-5]. In [4] authors identified properties of LRF Hokuyo URG-04LX in detail. Measuring principle of this rangefinder is similar to UTM-30LX type.

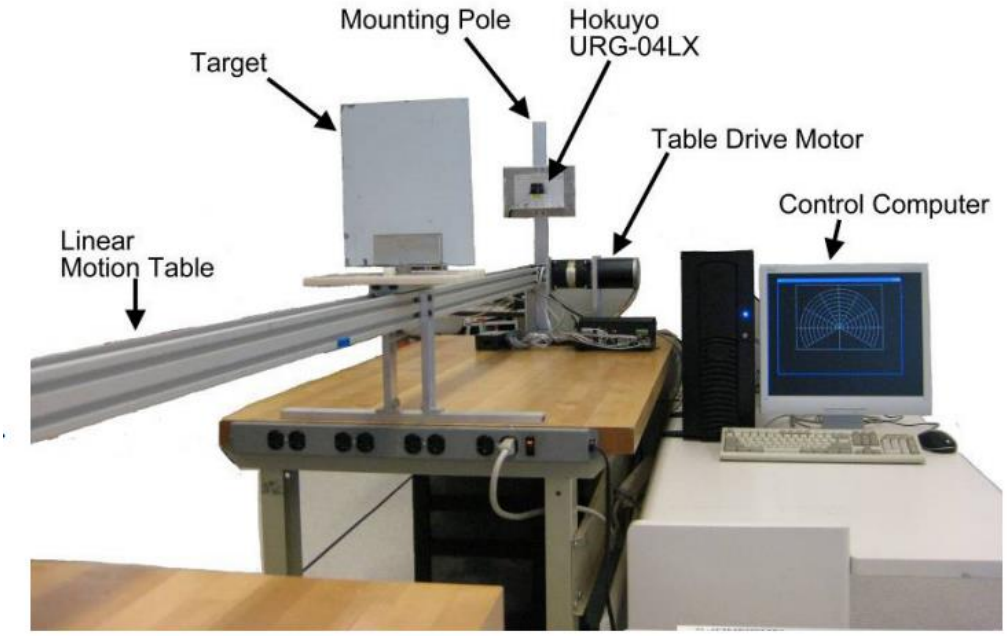

Fig.1. Setup for laser parameter measurement [4]

According to their results there is a Warm-up time of 80 minutes before the measurements stabilize as well as an error dependence on the type of the surface measuring (Fig 2.).

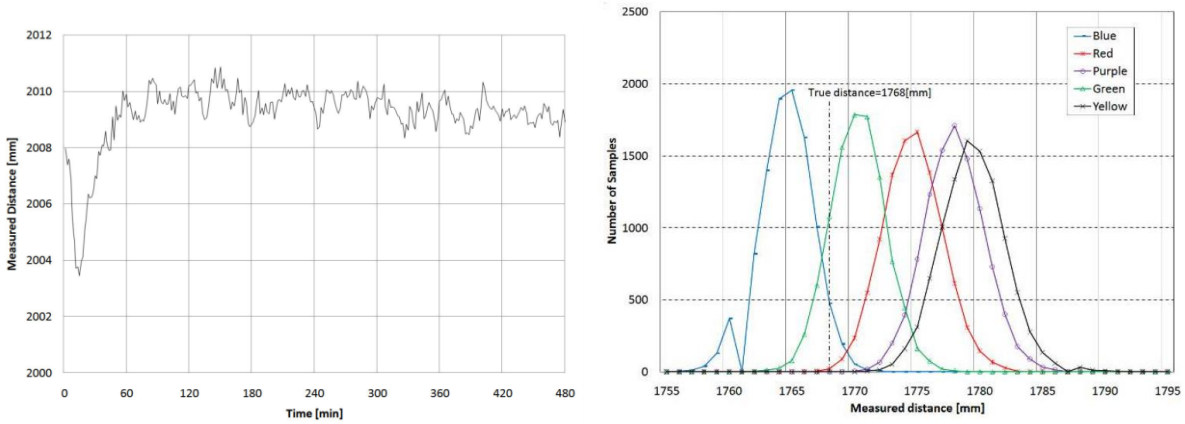

Fig 2. Parameters of LRF Hokuyo URG-04LX, warm up time (left) and distance difference on different surfaces (right) [4]

In [6] a picture of a wall measured with LRF Hokuyo URG-04LX was taken using a camera without an infrared filter. A ruler fixed on the wall was used to determine the beam diameter as shown in Fig. 3.

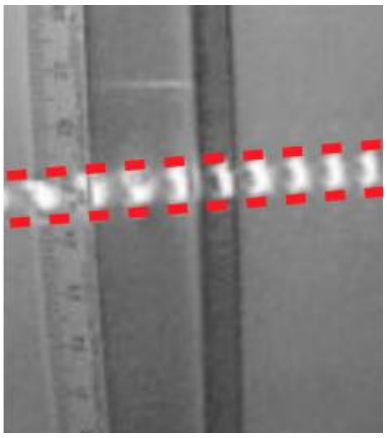

Fig 3. Laser beam pattern measured on a wall [6]

Probabilistic model creation

The Errors in measurement may significantly affect data interpretation and subsequent procedures. In mobile robotics, this can lead to destruction of robot, damage of objects or human injuries[10]. That is why it is needed to determine the type and size of errors in measurement as accurately as possible. In determining of laser rangefinder's errors, it is suitable to utilize the parameters that were specified by the manufacturer. However, these parameters are defined for specific conditions. In the case of mobile robotics such conditions may not been always respected. Hence it is needed to perform the measurements, which will determine rangefinder's parameters[8]. While the researchers in [4] and [6] focused mainly on distance error, in this work, we focused on the accuracy of measurement in respect of laser beam's rotation in space.

The result of these parameters is a probabilistic model. The concept of proposed model is derived from the model of Hokuyo URG-04LX used in [4]. This concept is focused on two basic parameters of rangefinder. The first parameter is derived from measurement's accuracy, e.g. stability of measured distances within the repeated measurement without the change in measurements conditions. The results of this parameter were already published in [7] and were very similar to [4]. Second parameter is an accuracy of measurement in respect of laser beam's rotation in space.

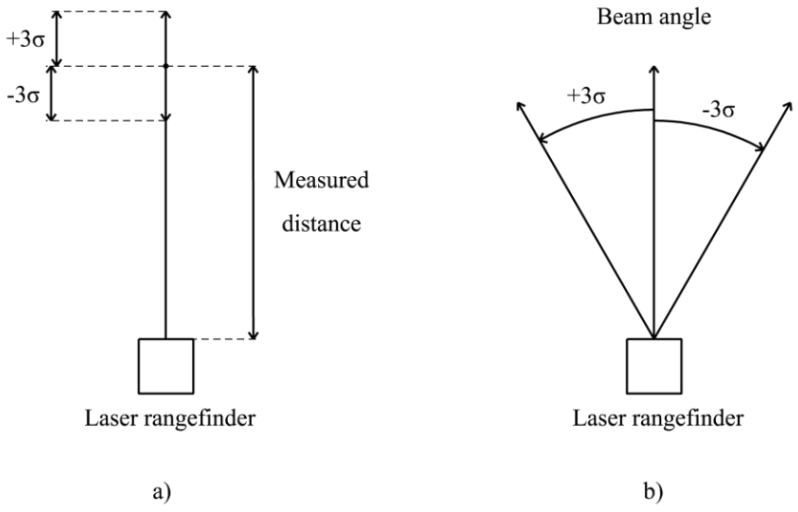

Fig 4. Parameters of LRF used in probabilistic model

The value of this parameter could be measured directly by taking picture as in [6]. But this method requires costly hardware and its result are questionable, because it can't determine whether the nearest beams found in consecutive measurements belongs to the same beam index in measurements. In our work, we used different approach. The LRF suffers from an error on the boundary of two objects named mixed pixel. This error arises when the reflected energy is distributed between these two objects, and the resulting distance is somewhere between these objects. Thus, when the heading of the laser beams between two consecutive measurements differ the location of mixed pixel should differ too. This error was used to determine the second parameter of proposed model.

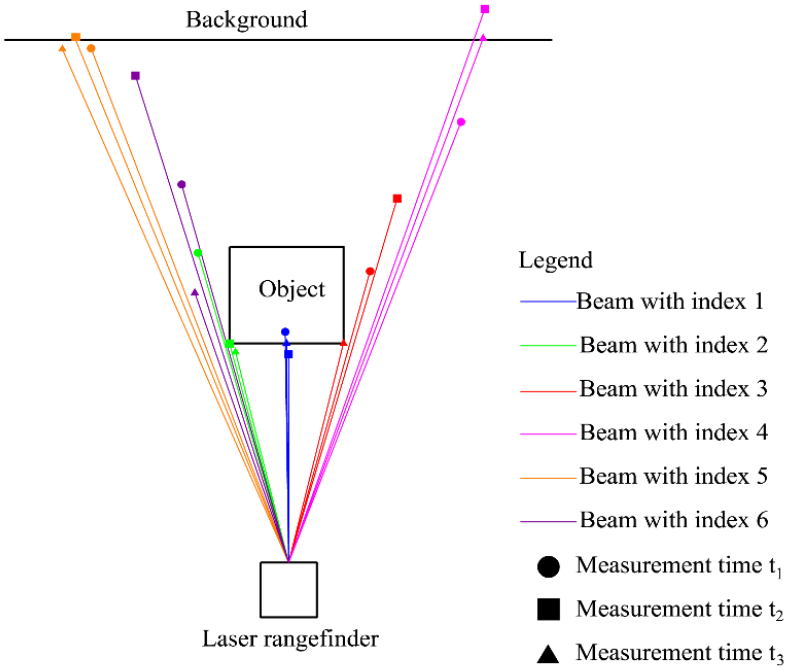

Fig 5. Principle of mixed pixel occurrence

Identification of mixed pixels can be used for determination of laser beam angle distribution. At the beginning, the boundary points of measured object are determined. At first, average standard deviation in measured distances for individual beams is computed (Fig. 6b). Adjacent beams without the sudden step in standard deviation correspond to the objects. The last beams of which standard deviation is under the threshold are boundary beams, i.e. boundary points (red dots at Fig. 6b). Beams where the standard deviation is different from the average standard deviations of the corresponding object are characterized by mixed pixels. These beams are consequently analyzed.

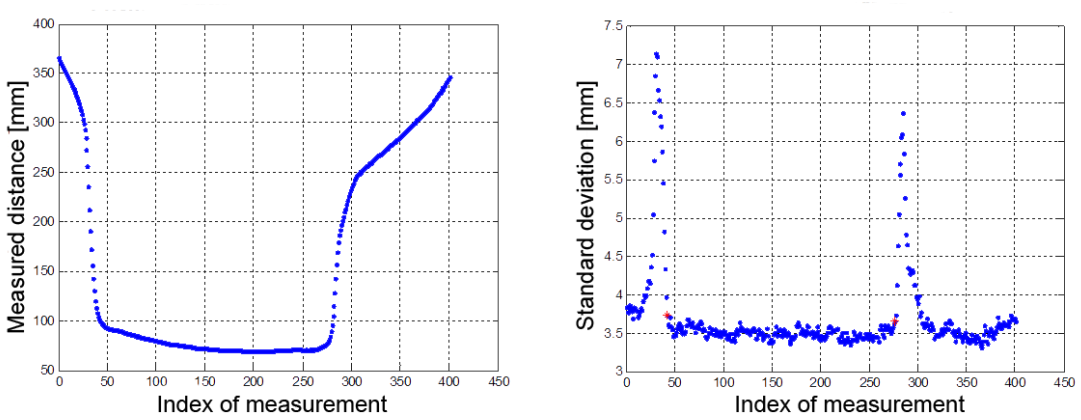

Fig 6. Average distance for individual laser beams measured on an object (a) and its corresponding standard deviation (b)

Analysis consists of the determination of ratio between the measurements on object and mixed pixels occurrence. The results are shown in Fig. 7. It is clear that seven adjacent beams to boundary beam securely cover the area of mixed pixels occurrence.

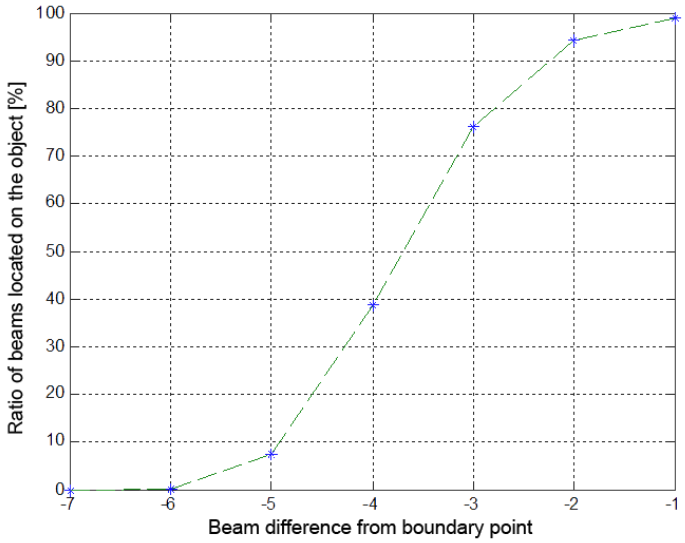

Fig 7. Ratio between the measurement located on object and as a mixed pixel.

Based on the frequencies of mixed pixel occurrence derived from this analysis variance of laser beam angle is determined.

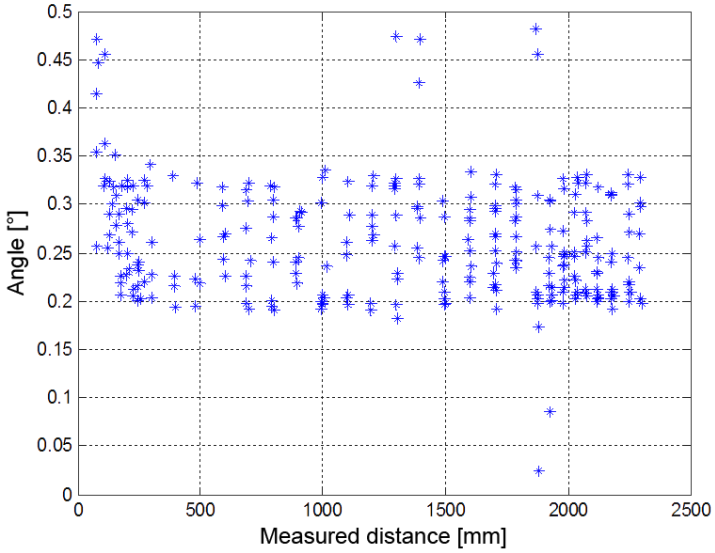

Fig 8. Variance of laser beam angle calculated for different measured distance and relative position between laser and object.

Resultant standard deviation was calculated as an average from the obtained values in Fig 8. and it is equal to σ_r =0.3616°. The model can be expressed as:

$$f(x,y) = \frac{1}{2\pi\sqrt{\sigma_x^2\sigma_y^2}} e^{-\left(\frac{(x-\mu_x)}{2\sigma_x^2}+\frac{(y-\mu_y)}{2\sigma_y^2}\right)}$$
$$\sigma_y = \tan(\sigma_r)x \qquad (1)$$

This model is dependent on measured distance (Fig. 9), which better corresponds to the characteristics of used LRF. However, as it can be seen in Fig 8, standard deviation of laser beam angle increases with decreasing measured distance. Therefore, Hokuyo LRF was submitted to further analysis and the model was extended.

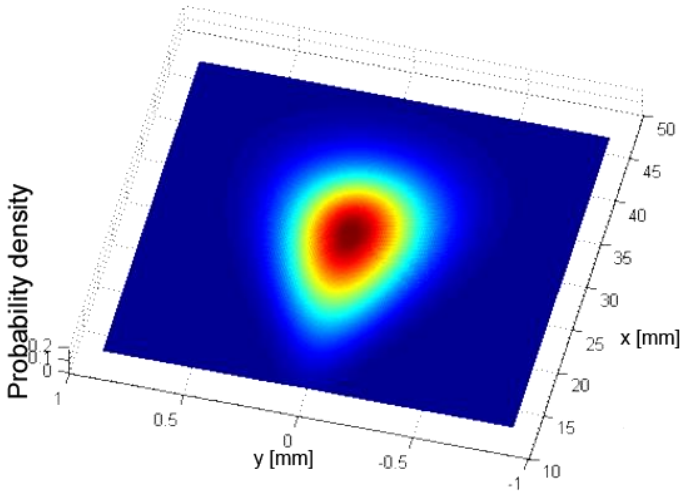

Fig 9. Probabilistic laser beam model based on equation (1).

The next concept of Hokuyo LRF model is focused on three parameters. The first two parameters are derived from the previous concept. However, in this case the second parameter was determined on the basis of new experiment. This parameter is defined as the value of accuracy concerning the distribution of laser beam angle and in this case, it also takes into account the width of the laser beam. The real width of the laser beam is constant at the same distance measurement, but it is distributed by some probability in the space due to inaccuracies in the sensor hardware. In the case when the width of the laser beam is neglected, the distribution of the laser beam angle is illustrated in Fig. 10. Angles α_{e1}, α_{e2}, α_{e3}, and α_{e4} represent the variance in laser beam angle, which is dependent on the measured distance. It is evident that influence of the laser beam width increases with decreasing measured distance.

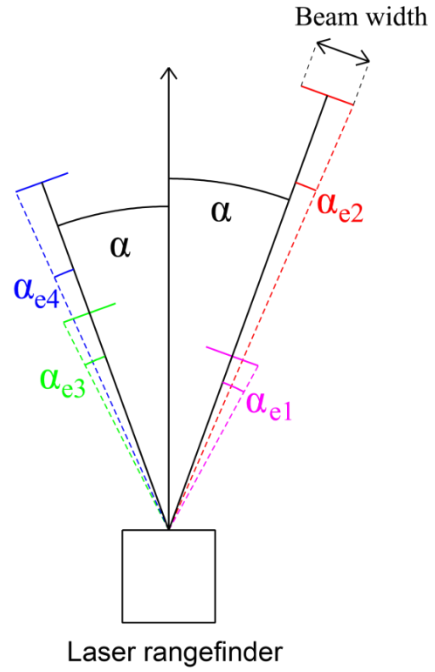

Fig 10. Variance of laser beam with marked beam width

It is clear that the variance of laser beam angle is greater at small distances. For this reason, such part of the measurements will be taken into account, where the influence of the laser beam width on the distribution of laser beam angle is significant. Influence of the laser beam width a on the variance of laser beam angle α is illustrated in Fig. 11. The situation in Fig. 11 describes the measurement, when the laser beam l'_2 seemingly measures distance to the object. In fact, it should not fall on this object and the measurement in this angle should include measurement to the background object. The whole issue is caused due to the laser beam width a and due to the variance of laser beam angle α. As it can be seen, influence of the laser beam width on the variance of the laser beam angle is not only function of the measured distance, but it is also the function of the relative position between LRF and measured object. This is expressed by the angle β, which represents the angle between the beam perpendicular to the object l_0 and the beam, which represents the boundary of the object l_1. However, due to the inaccuracies of the measurement (caused by the above-described effects), the boundary of the object can be represented by the beam l_2 – virtual boundary of the object. The difference between α and α' is that α' is not taking into account the width of the laser beam. Easier said, if the model uses only α' it is the second concept of LRF model. If the model uses α, it is the third concept of LRF model, because α is derived from α' and a.

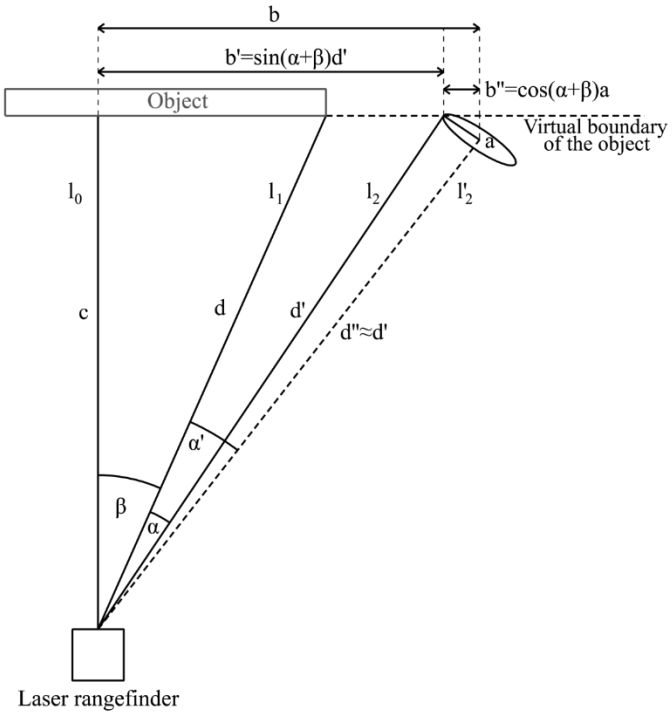

Fig 11. Principle of laser beam variance calculation with beam with taken into account.

It is clear that:

$$b = b' + b'' \tag{2}$$

By the expressions of individual sinuses in the triangles:

$$\sin(\alpha' + \beta) = \sin(\alpha + \beta) + \cos(\alpha + \beta)\frac{a}{d'} \tag{3}$$

There are two unknown variables in the equation (6) – width of the angle *a* and angle *α*. Seeing that the influence of the laser beam width decreases with increasing measured distance, it can be determined from the measuring of such distance, where this influence is negligible. For this reason, distributions in laser beam angle in Fig. 8 have been divided into two sets. First set contained measurements over the distance of 500 mm and the second set contained measurements under the distance of 500 mm. The angle *α* was determined on the basis of the first set (assumption that there is no influence of the laser beam width) and it is equal to 0.2473°. When compared to the angular resolution of the Hokuyo LRF, it may seem that two adjacent beams may be replaced in some cases by each other. However, this has not been confirmed by any experiment. And therefore, it appears that the variance of the laser beam angle consists of two parts. The first part is represented by constant variance of angle in whole measurement and second part is represented by variance of angle in individual laser beams. According to this assumption, variance of angle in individual laser beams is not one that would cause the exchange of adjacent beams. However, to confirm this assumption it is necessary to realize further experiments, which are not included in this article.

Regression curve defined by the method of least squares was used for determining the unknown laser beam width *a*:

$$min = \left[sin(\alpha + \beta) + cos(\alpha + \beta)\frac{a}{d'} - sin(\alpha' + \beta) \right]^2 \tag{4}$$

The minimum of the regression curve for the data shown in Fig. 12 is at *a* equal to 0.135 mm.

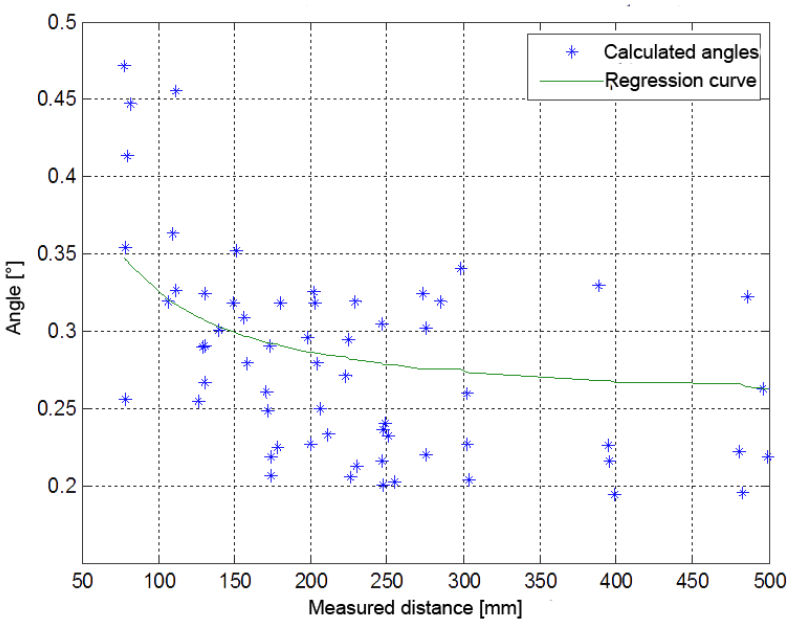

Fig 12. Variance of laser beam angle at short distances with regression curve that characterize the variance with beam width taken into account.

Resulting probabilistic model of Hokuyo LRF:

$$f(x,y)=\frac{1}{2\pi\sqrt{\sigma_x^2\sigma_y^2}}e^{-\left(\frac{(x-\mu_x)}{2\sigma_x^2}+\frac{(y-\mu_y)}{2\sigma_y^2}\right)}$$

$$\sigma_y = a + tan(\sigma_r)x \qquad (5)$$

Where a is laser beam width equal to 0.135 mm, σ_r is the standard deviation in laser beam angle equal to 0.2473°, and σ_r is standard deviation in the direction of measured distance and it is equal to 5.6894 mm [7]. Resulting model is shown in Fig. 13.

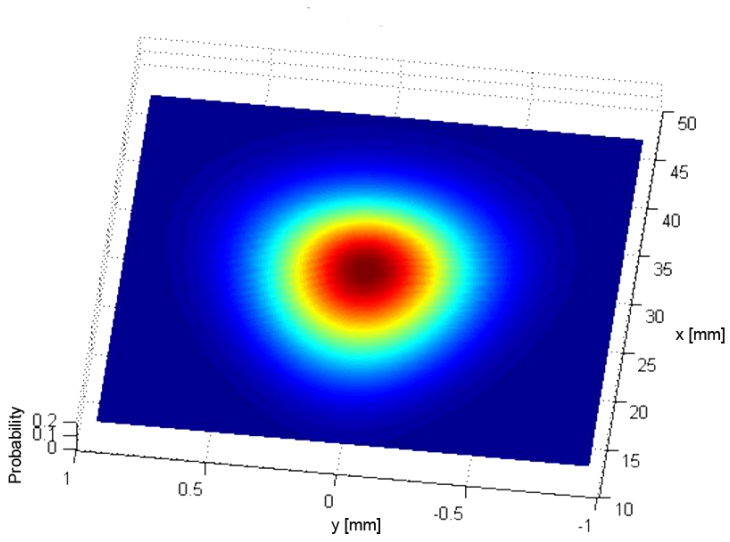

Fig 13. Final probabilictic model of LRF Hokuyou UTM30-LX

Conclusions

Before using the data from the sensors in mobile robotics, it is very important to understand their interpretation. Therefore, different models of sensors are usually used. We were not satisfied with existing models of Hokuyo type LRF. They were analyzed and the conclusion was that neither of them reflects the real nature of the measurement or expensive calibration equipment is needed for the estimation. Therefore, a new model of such sensor was created. It considers the width of the beam and it can be created without any other equipment.

Acknowledgments

This work was supported by national grants VEGA 1/0065/16 and VEGA 1/0752/17

References

[1] K. Konolige, J. Augenbraun, N. Donaldson, C. Fiebig and P. Shah, “A low-cost laser distance sensor”, in Proc. IEEE International Conference on Robotics and Automation, 2008, pp. 3002-3008.

[2] S. M. Nejad and S. Olyaee, “Comparison of TOF, FMCW and Phase-Shift Laser Range-Finding Methods by Simulation and Measurement”, Quartarly Journal of Technology & Education, vol. 1, no. 1, pp. 11-18, Autumn 2006.

[3] P. Labecki, M. Nowicki and P. Skrzypczynski, “Characterization of a compact laser scanner as a sensor for legged mobile robots”, Management and Production Engineering Review, vol. 3, no. 3, pp. 45-52, October 2012.

[4] Y. Okubo, C. Ye and J. Borenstein, “Characterization of the Hokuyo URG-04LX laser rangefinder for mobile robot obstacle negotiation”, in Proc. Unmanned Systems Technology XI, 2009, pp. 1-10.

[5] J. Tuley, N. Vandapel and M. Hebert, “Analysis of Artifacts in 3-D LADAR Data”, in Proc. IEEE International Conference on Robotics and Automation, 2005, pp. 2203-2210.

[6] F. Pomerleau, A. Breitenmoser, M. Liu, F. Colas, R. Siegwart. “Noise characterization of depth sensors for surface inspections.” in 2nd International Conference on Applied Robotics for the Power Industry (CARPI), 2012, Zurich, Switzerland. 2012, <10.1109/CARPI.2012.6473358>. <hal-01142707>

[7] M. Dekan, F. Duchoň, L. Jurišica and A. Vitko, "Probabilistic Model of Laser Rangefinder," AD ALTA: Journal of Interdisciplinary Research, vol. 1, no. 2, pp. 151-155, 2011.

[8] Vagaš, M., M. Sukop, and J. Semjon. "The calibration issues of 3D vision system by using two 2D camera sensors." International Scientific Herald 3.2 (2012): 264-237.

[9] Virgala, Ivan, and Peter Frankovský, Mária Kenderová. "Friction Effect Analysis of a DC Motor." American Journal of Mechanical Engineering 1.1 (2013): 1-5.

[10] I. Virgala, M. Kelemen, E. Prada and R. Surovec, "Motion analysis of snake robot segment," 2013 IEEE 11th International Symposium on Applied Machine Intelligence and Informatics (SAMI), Herl'any, 2013, pp. 145-148. doi: 10.1109/SAMI.2013.6480963

[11] Loncová, Z., Hargaš, L., Koniar, D., Hrianka, M., & Simonová, A. (2015). Parameters measurement of the object in a video sequence. IFAC-PapersOnLine, 48(4), 211-214.